Journal of Genetics and Genomics 48 (2021) 167–171

Contents lists available at ScienceDirect

Journal of Genetics and Genomics

Journal homepage: www.journals.elsevier.com/journal-of-genetics-and-genomics/

Letter to the editor

A custom-designed panel sequencing study in 201 Chinese patients with craniosynostosis revealed novel variants and distinct mutation spectra

Craniosynostosis is a rare disease in which one or more of the cranial sutures in an infant skull prematurely fuses by turning into bone, with a prevalence of 1 in 2,000–2,500 individuals from reports in Western countries (Wilkie et al., 2017). It may restrict the growth of the brain, leading to some degree of morphological and functional abnormalities, and may affect the neurocognitive function of infants (Lattanzi et al., 2017). Genetic variants underlying craniosynostosis have been identified in cohort studies in Western populations, including the UK (Kan et al., 2002; Wilkie et al., 2010, 2017), Australia (Roscioli et al., 2013; Lee et al., 2018), and Spain (Paumard-Hernández et al., 2015). However, non-Western populations have been substantially understudied. In China, with a population size of 1.4 billion, only a few case reports were found in the literature (Chen et al., 2013; Ke et al., 2015). We carried out a custom-designed 17-gene panel sequencing study in a cohort of 201 Chinese patients with craniosynostosis to explore the mutation spectrum and to test the diagnostic utility of the gene panels in Chinese patients (Table S1).

In our 201-patient cohort, 85 (42.3%) and 99 (49.3%) patients were clinically diagnosed with syndromic and nonsyndromic craniosynostosis, respectively, and the remaining 17 patients could not be clearly classified. We identified 51 different pathogenic/likely pathogenic variants in 105 patients, with a diagnostic yield of 94.1% (80/85) in patients with syndromic craniosynostosis and 18.2% (18/99) in patients with nonsyndromic craniosynostosis, higher than that in the UK (Wilkie et al., 2017) (69% for syndromic and 5% for nonsyndromic craniosynostosis), Australia (Roscioli et al., 2013) (71.0% of syndromic and 3.4% of nonsyndromic craniosynostosis), and Korea (Ko et al., 2012) (52.5% of syndromic and 17.1% of nonsyndromic craniosynostosis). In general, the diagnostic yield of the custom-designed 17-gene panel in the cohort of Chinese patients with craniosynostosis with no prior genetic testing was high (52.2%, 105/201, Fig. 1A; see Tables S2 and S3 for detailed information of solved and unsolved patients, respectively). The diagnostic rate of hot spot genes (*FGFR1-3, TWIST1, EFNB1, ERF,* and *TCF12*) was 51.2% (103/201), higher than that in the UK (18.2%, 121/666), Australia (36.2%, 228/630), and Korea (19.1%, 21/110), which further indicates the gene panel has a high diagnostic yield. It has to be noted that not all the important genes related to craniosynostosis were included in this panel. For example, *SMAD6* is frequently mutated in metopic and sagittal synostosis and *CDC45* is related to an incomplete feature of craniosynostosis in Meier-Gorlin syndrome (Wilkie et al., 2017) and 22q11.2 deletion syndrome (Unolt et al., 2020). These genes should be considered in future research based on whole-exome sequencing, and the efficiency of the number of genes included in panel can also be evaluated.

Concurrently, we observed that multiple (29/86) and bilateral coronal (23/86) synostosis was most frequent in patients with syndromic craniosynostosis, whereas isolated sagittal (37/98) and unilateral coronal (32/98) synostosis were most frequent in patients with nonsyndromic craniosynostosis. The diagnostic yields of different types of suture fusion varied widely, from 79.1% (34/43) for multiple synostoses to 0% (0/40) for sagittal suture fusion (Fig. 1A). The 51 identified variants were distributed in 9 genes (*EFNB1*, *ERF*, *FGFR1*, *FGFR2, FGFR3*, *POR*, *TCF12*, *TGFBR2*, and *TWIST1*). The predicted functional changes of these 51 variants could be classified as 35 missense, six nonsense, three splicing, six frameshift, and one in-frame deletion (Table S4).

Among the 51 pathogenic or likely pathogenic variants, 36 had been reported in the literature or databases (e.g., ClinVar, HGMD), whereas 15 variants distributed in *TWIST1* (7), *TCF12* (5), *FGFR2* (2), and *TGFBR2* (1) are newly reported in this study (Table 1). This percentage (29.4%, 15/51) is much higher than that of other large studies (11.1–21.3%) (Roscioli et al., 2013; Paumard-Hernández et al., 2015; Lee et al., 2018), suggesting studies in non-Western patients could substantially expand the mutation spectrum in rare diseases such as craniosynostosis.

Most of the variants identified in *TWIST1* and *TCF12* were novel (80%, 12/15), in which six frameshift variants and three nonsense variants were loss-of-function or located in the reported functional regions, and three missense variants were predicted to be damaging by at least two in silico tools, consistent with the pathological mechanism of haploinsufficiency in both genes. Meanwhile, the *de novo* origin increases the probable pathogenicity of *TCF12* c.1736G>A and *TWIST1* c.329G>A. Of four patients with a variant inherited from one parent, we successfully recontacted two families for further information. The mother of proband-99 was confirmed to have a mild unilateral synostosis of the coronal suture on computed tomography (CT) imaging of the skull (Fig. S1). The father of proband-126 showed mild exophthalmos and midface hypoplasia, as shown in front and side facial photos. Hence, the pathogenicity of the respective variants (*TWIST1* c.153delG and *TWIST1* c.421G>A) was strengthened by the confirmation of mutation-positive parents, consistent with the pathogenic evidence PP1 of ACMG (Richards et al., 2015).

Although the gain-of-function variants in *FGFR2* have been well explored in the past 25 years, this study still found a novel double-mutant p.N265K/A266D and in-frame deletion p.G272del. A double-mutant p.N265K/A266D on *FGFR2* (the two variants were

https://doi.org/10.1016/j.jgg.2020.11.004

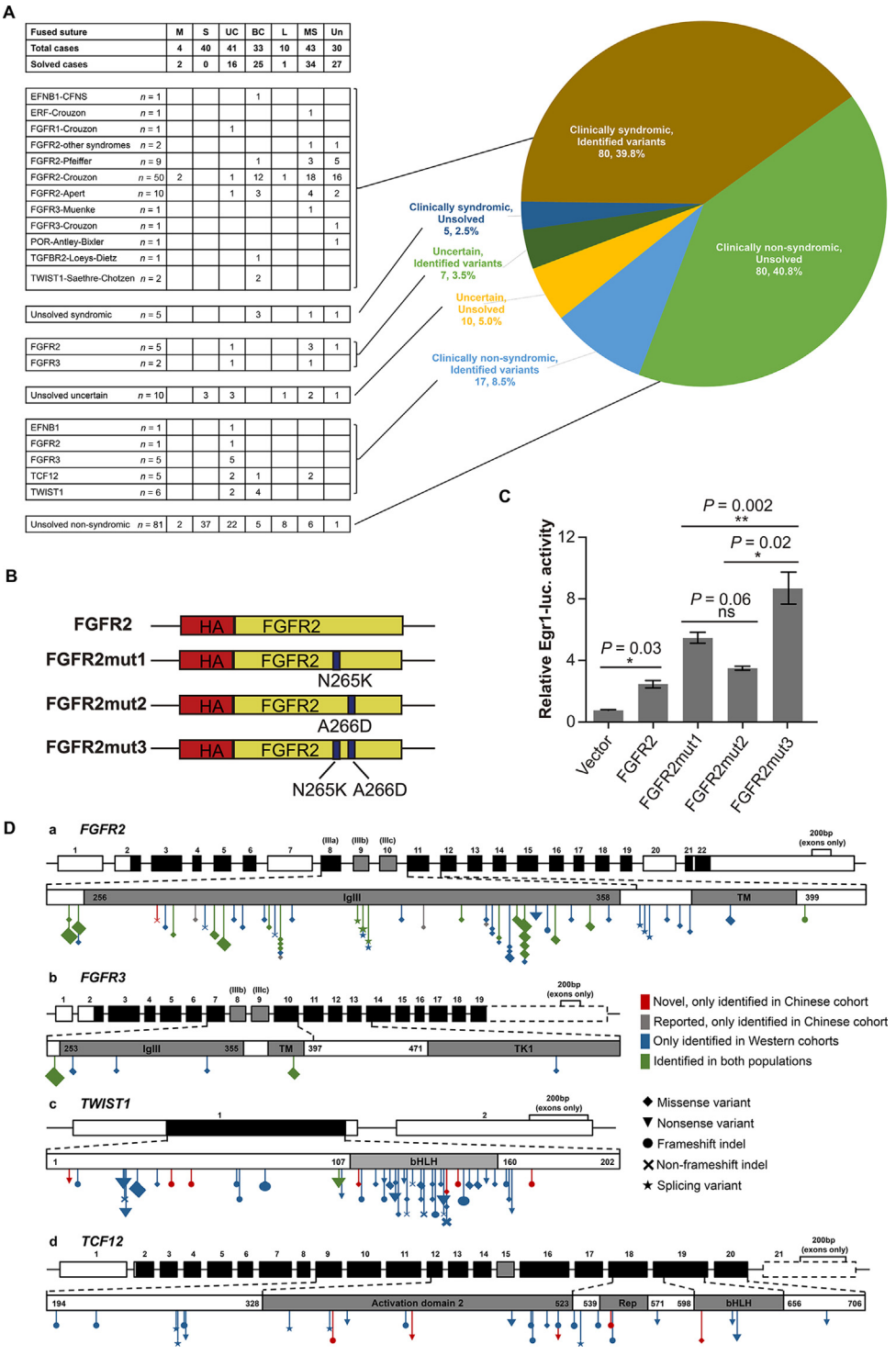

Fig. 1. Summary of genetic diagnosis, functional validation, and mutation spectra. **A**: Clinical diagnosis and genetic causes of craniosynostosis in the Chinese cohort of this study ($n = 201$). The pie chart on the right shows a broad classification based on clinical symptoms and identification of genetic causes in this study. The grid on the left provides a more detailed breakdown as per the pattern of fused sutures and clinical diagnosis. CFNS, craniofrontonasal syndrome. Abbreviations for different suture fusions are as follows: S, sagittal; M, metopic; UC, unilateral coronal; BC, bilateral coronal; L, unilateral or bilateral lambdoid; MS, multiple suture fusion excluding bilateral coronal or lambdoid; Un, uncertain pattern. **B**: Schematic diagram of FGFR2 domain mutations. A series of mutant expression vectors based on the wild-type FGFR plasmid were constructed, including FGFR2 p.N265K, FGFR2 p.A266D, and FGFR2 p.N265K/A266D. **C**: Effects of FGFR2 domain mutations on MAPK activity in HEK293T cells, measured using the *Egr1*-Luciferase report system. We performed dual-luciferase reporter assay with Egr1-luciferase (Balamotis et al., 2009) and Renilla in HEK293T cells, showing wild-type FGFR2 could activate the MAPK signaling pathway consistent with previous reports (Powers et al., 2000). Data are presented as means ± SEM. Statistical significance was determined using the two-tailed Student's *t*-test. *, $P < 0.05$. **, $P < 0.01$. ***, $P < 0.001$. **D**: Population comparison of mutation spectra in *FGFR2*, *FGFR3*, *TWIST1,* and *TCF12*. Different mutation types are presented in different shapes. The size of shape symbols is approximately proportional to the number of cases of the variant (see details in Tables S6−S9). Different colors indicate whether the variants were found in Chinese or Western patients. In the genomic structures, coding regions are in black and the alternatively spliced exons are in gray. Exon 19 of *FGFR3* and exon 21 of *TCF12* are not shown in exact length because of the limitation of the frame size. Parts of the encoded protein are shown schematically below the genomic structure, with domains in dark gray. To be consistent with other mutation types, splicing variants are marked at their approximate splicing location in the protein schematic. SEM, standard error of the mean; ns, no significance.

Table 1
Summary of 15 novel variants.

No.	Sex	Diagnosis	Genomic change (GRCh37/hg19)	Gene[a]	Exon	Nucleotide changes	Amino acid alteration	Functional change	Inheritance[b]	Evidence of pathogenicity	Classification
35	F	Nonsyndromic	chr7:g.19156922G>T	*TWIST1*	exon1	c.23C>A	p.S8*	Stop gain	Maternal	PVS1, PM2, PP3, PP4	Pathogenic
141	M	Nonsyndromic	chr7:g.19156803_19156813del	*TWIST1*	exon1	c.132_142del	p.R44fs	Frameshift deletion	*De novo*	PVS1, PS2, PM2, PP4	Pathogenic
99	M	Nonsyndromic	chr7:g.19156792del	*TWIST1*	exon1	c.153del	p.G51fs	Frameshift deletion	Maternal	PVS1, PM2, PP4	Pathogenic
55	F	Nonsyndromic	chr7:g.19156616C>T	*TWIST1*	exon1	c.329G>A	p.R110Q	Missense	*De novo*	PS2, PM1, PM2, PM5, PP3, PP4	Pathogenic
126	F	Nonsyndromic	chr7:g.19156524C>T	*TWIST1*	exon1	c.421G>A	p.D141N	Missense	Paternal	PM1, PM2, PP1, PP3, PP4	Likely pathogenic
27	F	Nonsyndromic	chr7:g.19156509dup	*TWIST1*	exon1	c.434dup	p.K145fs	Frameshift insertion	*De novo*	PVS1, PS2, PM2, PP4	Pathogenic
191	F	Saethre-Chotzen	chr7:g.19156435dup	*TWIST1*	exon1	c.510dup	p.K171fs	Frameshift insertion	Uncertain	PVS1, PM2, PP4	Likely pathogenic
183	M	Nonsyndromic	chr15:g.57543550delA	*TCF12*	exon14	c.1117del	p.T373fs	Frameshift deletion	Maternal	PVS1, PM2, PP4	Pathogenic
201	F	Nonsyndromic	chr15:g.57545617C>G	*TCF12*	exon15	c.1418C>G	p.S473*	Stop gain	*De novo*	PVS1, PS2, PM2, PP3, PP4	Pathogenic
88	M	Nonsyndromic	chr15:g.57554365C>A	*TCF12*	exon17	c.1541C>A	p.S514*	Stop gain	*De novo*	PVS1, PS2, PM2, PP3, PP4	Pathogenic
32	F	Nonsyndromic	chr15:g.57555366_57555370del	*TCF12*	exon18	c.1639_1643del	p.K547fs	Frameshift deletion	*De novo*	PVS1, PS2, PM2, PP4	Pathogenic
195	F	Nonsyndromic	chr15:g.57565290G>A	*TCF12*	exon18	c.1808G>A	p.R603Q	Missense	*De novo*	PS2, PM1, PM2, PP3, PP4, BP1	Likely pathogenic
17	M	Crouzon	chr10:g.123279635_123279637 delinsTCC	*FGFR2*	exon7	c.[795T>G; 797C>A]	p.[N265K; A266D]	Missense	Uncertain	PS3, PM1, PM2, PP3, PP4	Pathogenic
125	F	Crouzon	chr10:g.123279615_123279617del	*FGFR2*	exon7	c.815_817del	p.G272del	In-frame deletion	Uncertain	PM1, PM2, PP3, PP4	Likely pathogenic
198	F	Crouzon	chr10:g.123279615_123279617del	*FGFR2*	exon7	c.815_817del	p.G272del	In-frame deletion	*De novo*	PS2, PM1, PM2, PP3, PP4	Pathogenic
106	M	Loeys-Dietz	chr3:g.30715601G>A	*TGFBR2*	exon5	c.1259G>A	p.G420E	Missense	*De novo*	PS2, PM1, PM2, PM5, PP3	Pathogenic

[a] The transcript numbers are shown in Table S1.
[b] Paternal/maternal: variant is inherited from the father/mother; uncertain: biospecimen unavailable for at least one of the parents.

on the same allele, Fig. S2) was detected in proband-17, of which *FGFR2* p.N265K and *FGFR2* p.A266D were classified as pathogenic and uncertain, respectively. We further tested whether the double *FGFR2* mutant demonstrated a synergistic action of the two missense variants by *in vitro* dual-luciferase reporter assay. We showed that wild-type FGFR2 can activate the MAPK signaling pathway, which is consistent with previous reports (Lenton et al., 2005), and each of the *FGFR2* mutations (*FGFR2* p.N265K and *FGFR2* p.A266D) could significantly facilitate the FGFR2 transcriptional activity, and the double-mutant showed a synergistic effect on Egr1-luciferase activity (Fig. 1B and 1C). The patient visited Huashan Hospital at the age of six years with the typical Crouzon clinical manifestations of midface hypoplasia, bilateral coronal suture fusion, and exophthalmos. The other novel mutation in *FGFR2* is an in-frame deletion p.G272del, also located in the IgIII domain. The deletion of the adjacent 273 residues (*FGFR2* p.D273del) was reported in a patient diagnosed with Pfeiffer type II (Priolo et al., 2000), which provided strong evidence for the pathogenicity of *FGFR2* p.G272del.

Notably, a *de novo* heterozygous variant p.G420E in *TGFBR2* was detected in proband-106, who has bilateral coronal synostosis, mild brachycephaly, and hypertelorism. This patient was initially diagnosed with nonsyndromic coronal craniosynostosis. Because mutations in *TGFBR2* reportedly cause Loeys-Dietz syndrome (Loeys et al., 2005), we rechecked and found that the patient had slender fingers, cleft palate, and tall stature, consistent with the clinical characteristics of Loeys-Dietz syndrome. The clinical diagnosis of this patient was therefore corrected. In addition, considering the *TGFBR2* mutation was also associated with thoracic aortic aneurysms and dissections, the patient was referred for echocardiography, CT, MRI, and clinical examination of the thoracic aorta, which confirmed normal dimensions. The patient was advised to conduct follow-up checks regularly.

Previous studies have shown that the mutation spectra of craniosynostosis are variable in different regions (Paumard-Hernández et al., 2015). To learn more about the global clinical diagnostic utility of the knowledge mainly from the Western populations, we compared the mutation spectra of the Chinese cohort with three large cohorts from the Western countries, including the UK, Australia, and Spain (hereafter referred to as the Western cohorts, Table S5). The most frequently mutated genes were the same (*FGFR2, FGFR3, TWIST1, TCF12*), explaining 94.3% (99/105) of solved patients in the present study and 85.5% (470/550) in the Western cohort. Moreover, the proportion of *FGFR2* mutation was significantly higher in the Chinese than in the Western cohorts (73.3% *vs.* 46.7%, respectively, $P = 4.4E-07$), whereas the proportion of *FGFR3* mutation was significantly lower (8.6% *vs.* 17.1%, respectively, $P = 0.028$). In the mutation spectrum of each gene, the patterns of *FGFR2* and *FGFR3* are similar in Chinese and Western cohorts, whereas patterns of *TWIST1* and *TCF12* are more different (Fig. 1D; Tables S6–S9). The over-representation of *FGFR2* mutation in this study is likely to be caused by sampling bias at the plastic surgery unit, where the sample collection took place, as patients with *FGFR2*-related syndromes (Crouzon, Pfeiffer, Apert, and so on) are more likely to seek plastic surgery correction (Goos and Mathijssen, 2019). The high diagnostic rate in this study may also be due to the same reason.

We further explored the genotype-phenotype correlation based on a questionnaire of clinical features (Table S10), particularly of patients with *FGFR2* mutations, in which we have a relatively large sample size (Table S11). We found that the respiratory system was significantly more frequently affected in *FGFR2*-positive patients than in *FGFR2*-negative patients (57.7% *vs.* 20.8%, respectively, $P = 6.0E-03$) (Table S12). Consistent with previous studies (Shotelersuk et al., 2002; Lajeunie et al., 2006), we found that several recurrent amino acid changes (p.C342S/W/R/Y, p.W290S/L/C and

splicing variants near c.940) were commonly associated with more severe features. More than 75% of the patients carrying these amino acid changes showed craniofacial abnormality, exophthalmos, or respiratory abnormality (Table S13). As for the clinical features associated with specific mutations, we found that patients with p.C342S/W/R/Y were less likely to have digit abnormality (P = 9.3E-03, Table S14), probably because p.C342R is actually the most common mutation in Pfeiffer syndrome. We also found that patients with the splicing variants near c.940 were more likely to have digit and foot abnormality (P = 5.4E-04 for the digit, P = 7.2E-03 for the foot, Table S14), probably because of the splicing variants' strong associations with Pfeiffer syndrome.

Taken together, by carrying out the first large-scale study on a cohort of patients with craniosynostosis in China, we showed that our custom-designed 17-gene sequencing panel could provide a high yield of diagnoses in Chinese patients with craniosynostosis. We also reported a substantial number of novel variants, expanding the mutation spectrum of craniosynostosis.

Conflict of interest

The authors declare they have no conflict of interest.

Acknowledgments

We are grateful to the families who participated in this study. We acknowledge the constructive comments on the manuscript from Dr. Yulan Lu (Children's Hospital of Fudan University, Shanghai, China), and all suggestions collected during the poster exhibition of ASHG 2019 Annual Meeting. We thank Prof. Lin Chen (Third Military Medical University, Chongqing, China) and Prof. Gang Wang (Fudan University, Shanghai, China) for providing FGFR2 wild-type plasmid and Egr1-Luciferase plasmid. This work was supported by the foundation of Shanghai municipal commission of Health and Family Planning (20174Y0088), the Shanghai Municipal Science and Technology Major Project (2017SHZDZX01), the CAS Interdisciplinary Innovation Team Project, and the NIHR Oxford Biomedical Research Centre Programme.

Supplementary data

Supplementary data to this article can be found online at https://doi.org/10.1016/j.jgg.2020.11.004.

References

Balamotis, M.A., Pennella, M.A., Stevens, J.L., Wasylyk, B., Belmont, A.S., Berk, A.J., 2009. Complexity in transcription control at the activation domain-mediator interface. Sci. Signal. 2, ra20.

Chen, C.-P., Huang, H.-K., Liu, Y.-P., Chern, S.-R., Su, J.-W., Wang, W., 2013. Pfeiffer syndrome with FGFR2 W290C mutation perinatally presenting extreme proptosis. Taiwan. J. Obstet. Gynecol. 52, 607−610.

Goos, J.A.C., Mathijssen, I.M.J., 2019. Genetic causes of craniosynostosis: an update. Mol. Syndromol. 10, 6−23.

Kan, S., Elanko, N., Johnson, D., Cornejo-Roldan, L., Cook, J., Reich, E.W., Tomkins, S., Verloes, A., Twigg, S.R.F., Rannan-Eliya, S., et al., 2002. Genomic screening of fibroblast growth-factor receptor 2 reveals a wide spectrum of mutations in patients with syndromic craniosynostosis. Am. J. Hum. Genet. 70, 472−486.

Ke, R., Yang, X., Ge, M., Cai, T., Lei, J., Mu, X., 2015. S267P mutation in FGFR2: first report in a patient with Crouzon syndrome. J. Craniofac. Surg. 23, 592−594.

Ko, J.M., Jeong, S.Y., Yang, J.A., Park, D.H., Yoon, S.H., 2012. Molecular genetic analysis of TWIST1 and FGFR3 genes in Korean patients with coronal synostosis: identification of three novel TWIST1 mutations. Plast. Reconstr. Surg. 129, 814e−821e.

Lajeunie, E., Heuertz, S., El Ghouzzi, V., Martinovic, J., Renier, D., Le Merrer, M., Bonaventure, J., 2006. Mutation screening in patients with syndromic craniosynostoses indicates that a limited number of recurrent FGFR2 mutations accounts for severe forms of Pfeiffer syndrome. Eur. J. Hum. Genet. 14, 289−298.

Lattanzi, W., Barba, M., Di Pietro, L., Boyadjiev, S.A., 2017. Genetic advances in craniosynostosis. Am. J. Med. Genet. A. 173, 1406−1429.

Lee, E., Le, T., Zhu, Y., Elakis, G., Turner, A., Lo, W., Venselaar, H., Verrenkamp, C.-A., Snow, N., Mowat, D., et al., 2018. A craniosynostosis massively parallel sequencing panel study in 309 Australian and New Zealand patients: findings and recommendations. Genet. Med. 20, 1061−1068.

Lenton, K.A., Nacamuli, R.P., Wan, D.C., Helms, J.A., Longaker, M.T., 2005. Cranial suture biology. Curr. Top. Dev. Biol. 66, 287−328.

Loeys, B.L., Chen, J., Neptune, E.R., Judge, D.P., Podowski, M., Holm, T., Meyers, J., Leitch, C.C., Katsanis, N., Sharifi, N., et al., 2005. A syndrome of altered cardiovascular, craniofacial, neurocognitive and skeletal development caused by mutations in TGFBR1 or TGFBR2. Nat. Genet. 37, 275−281.

Paumard-Hernández, B., Berges-Soria, J., Barroso, E., Rivera-Pedroza, C.I., Pérez-Carrizosa, V., Benito-Sanz, S., López-Messa, E., Santos, F., García-Recuero, I.I., Romance, A., et al., 2015. Expanding the mutation spectrum in 182 Spanish probands with craniosynostosis: identification and characterization of novel TCF12 variants. Eur. J. Hum. Genet. 23, 907−914.

Powers, C.J., McLeskey, S.W., Wellstein, A., 2000. Fibroblast growth factors, their receptors and signaling. Endocr. Relat. Canc. 165−197.

Priolo, M., Lerone, M., Baffico, M., Baldi, M., Ravazzolo, R., Cama, A., Capra, V., Silengo, M., 2000. Pfeiffer syndrome type 2 associated with a single amino acid deletion in the *PGFR2* gene. Clin. Genet. 58, 81−83.

Roscioli, T., Elakis, G., Cox, T.C., Moon, D.J., Venselaar, H., Turner, A.M., Le, T., Hackett, E., Haan, E., Colley, A., et al., 2013. Genotype and clinical care correlations in craniosynostosis: findings from a cohort of 630 Australian and New Zealand patients. Am. J. Med. Genet. C. Semin. Med. Genet. 163, 259−270.

Shotelersuk, V., Ittiwut, C., Srivuthana, S., Mahatumarat, C., Lerdlum, S., Wacharasindhu, S., 2002. Distinct craniofacial-skeletal-dermatological dysplasia in a patient with W290C mutation inFGFR2. Am. J. Med. Genet. 113, 4−8.

Richards, S., Aziz, N., Bale, S., Bick, D., Das, S., Gastier-Foster, J., Grody, W.W., Hegde, M., Lyon, E., Spector, E., et al., 2015. ACMG Laboratory Quality Assurance Committee. Standards and guidelines for the interpretation of sequence variants: a joint consensus recommendation of the American College of Medical Genetics and Genomics and the Association for Molecular Pathology. Genet Med. 17, 405−424.

Unolt, M., Kammoun, M., Nowakowska, B., Graham, G.E., Crowley, T.B., Hestand, M.S., Demaerel, W., Geremek, M., Emanuel, B.S., Zackai, E.H., et al., 2020. Pathogenic variants in CDC45 on the remaining allele in patients with a chromosome 22q11.2 deletion result in a novel autosomal recessive condition. Genet. Med. 22, 326−335.

Wilkie, A.O.M., Byren, J.C., Hurst, J.A., Jayamohan, J., Johnson, D., Knight, S.J.L., Lester, T., Richards, P.G., Twigg, S.R.F., Wall, S.A., 2010. Prevalence and complications of single-gene and chromosomal disorders in craniosynostosis. Pediatrics 126, e391−e400.

Wilkie, A.O.M., Johnson, D., Wall, S.A., 2017. Clinical genetics of craniosynostosis. Curr. Opin. Pediatr. 29, 622−628.

Yingzhi Wu[1]
Department of Plastic Surgery, Huashan Hospital, Fudan University, Shanghai 200040, China

Meifang Peng[1], Jieyi Chen[1]
State Key Laboratory of Genetic Engineering at School of Life Sciences, Fudan University, Shanghai 200011, China

CAS Key Laboratory of Computational Biology, CAS-MPG Partner Institute for Computational Biology, Shanghai Institute of Nutrition and Health, University of Chinese Academy of Sciences, Chinese Academy of Sciences, Shanghai 200031, China

Jinlong Suo
The State Key Laboratory of Cell Biology, CAS Center for Excellence in Molecular Cell Science, Shanghai Institute of Biochemistry and Cell Biology, Chinese Academy of Sciences, University of Chinese Academy of Sciences, Shanghai 200031, China

Sihai Zou
Department of Oral and Maxillofacial Surgery, Affiliated Hospital of Stomatology, Chongqing Medical University, Chongqing 401147, China

Chongqing Key Laboratory of Oral Diseases and Biomedical Sciences, Chongqing 401147, China

[1] These authors contributed equally to this work.

Yanqing Xu
Forest Ridge School of the Sacred Heart, Bellevue, WA 98006, USA

Andrew O.M. Wilkie
MRC Weatherall Institute of Molecular Medicine, University of Oxford, John Radcliffe Hospital, Oxford OX3 9DS, UK

Weiguo Zou
The State Key Laboratory of Cell Biology, CAS Center for Excellence in Molecular Cell Science, Shanghai Institute of Biochemistry and Cell Biology, Chinese Academy of Sciences, University of Chinese Academy of Sciences, Shanghai 200031, China

Xiongzheng Mu[**]
Department of Plastic Surgery, Huashan Hospital, Fudan University, Shanghai 200040, China

Sijia Wang[*]
CAS Key Laboratory of Computational Biology, CAS-MPG Partner Institute for Computational Biology, Shanghai Institute of Nutrition and Health, University of Chinese Academy of Sciences, Chinese Academy of Sciences, Shanghai 200031, China

Center for Excellence in Animal Evolution and Genetics, Chinese Academy of Sciences, Kunming 650223, China

[**] Corresponding author.
[*] Corresponding author.
E-mail addresses: cranio@vip.163.com (X. Mu), wangsijia@picb.ac.cn (S. Wang).

19 August 2020
Available online 30 December 2020